Journal of Alloys and Compounds 509 (2011) 8228–8234

Contents lists available at ScienceDirect

Journal of Alloys and Compounds

journal homepage: www.elsevier.com/locate/jallcom

Ab initio investigation of structures, electronic and thermodynamic properties for Li–Mg–H ternary system

Daixin Li, Tianran Zhang, Siqi Yang, Zhanliang Tao, Jun Chen*

Key Laboratory of Advanced Energy Materials Chemistry (Ministry of Education), Nankai University, Tianjin 300071, PR China

ARTICLE INFO

Article history:
Received 8 March 2011
Received in revised form 22 May 2011
Accepted 23 May 2011
Available online 30 May 2011

Keywords:
Li_2MgH_4
$LiMgH_3$
DFT
Structural prediction
Thermodynamic

ABSTRACT

A systematic consideration of the compounds made up of Li, Mg and H has been taken with respect to the structural, electronic, and thermodynamic properties, by means of density functional theory (DFT). Through the database mining approach, the ground state structures of $LiMgH_3$ and Li_2MgH_4 are identified to be *R*3*c* and *Pbam*, respectively. The Li–Mg–H ternary hydrides are insulators dominated by ionic bonds besides some covalent components between Mg and H. Energies of different formation pathways have been calculated at finite temperature. Hydrides synthesized from Li, Mg and H_2 possess obvious energetic advantage, but may be inhabited kinetically by pure phase separation. Thermodynamically reversible decomposition to LiH and MgH_2 brings about another issue for the actual preparation and stable existence of the ternary hydrides. Inserting H atoms to the sites of the ordered alloys with high electric density has been taken as another way to explore possible structures of this system. As H uptakes stepwise, the resulted compounds turn from conductors to insulators. The present results shed light on the design of Li–Mg–H ternary hydrides.

1. Introduction

Lithium, magnesium and hydrogen come out at the top of the lightweight elements and exhibit a variety of high-efficiency applications especially in the area of energy storage and conversion [1,2]. Lithium and magnesium are believed to have similar properties due to their diagonal situations on the periodic table. In terms of the practical hydrogen storage demand for fuel cells, many efforts have been currently aimed at exploring complex light-weight metal hydrides $A_m(MH_4)_n$ (A = Li, Na; M = Be, B, Al) [3,4], owing to their high gravimetric and volumetric hydrogen storage capacity. From this point of view, the Li–Mg–H ternary phases possess great potential. Recently, focuses have been expanded to multi-component hydrides, mainly including Li–Mg–N–H [5–7] or Li–Mg–B–H [8,9] systems. By mixing and reacting the binary metal hydrides with amides or borohydrides, the complex systems undergo a variety of competing reactions and reach different end products. Thus, the Li–Mg–H compounds may also exist as the by-products during the reactions of multiphase hydrides or as the mixed phases in doping Li (or Mg) into some Mg (or Li)-based hydrides.

On the other hand, Li, together with Mg, acts a significant role on rechargeable batteries [10]. Searching for high-performance lithium storage materials as electrodes has constantly attracted wide interest ever since the first commercialized rocking-chair cell by Sony Corporation [11]. Oumellal et al. presented the electrochemical reactivity of MgH_2 with Li that constitutes the first use of a metal-hydride electrode for Li-ion batteries [12]. A mixture of LiH and Mg has also been suggested as a negative electrode corresponding to the conversion reaction: $Mg + 2LiH \rightarrow MgH_2 + 2Li^+ + 2e$ [13]. Some voltage plateau during the charge–discharge traces was regarded to substances including Li, Mg and H, though the specific composition has not been verified. Thus, the Li–Mg–H ternary system plays a significant role in the areas related to high efficient energy storage and conversion. The Li–Mg–H ordered phases have a great potential to fulfill the needs of both lithium and hydrogen storage, and the gravimetric H and Li density is 8.8%, 20.6% for $LiMgH_3$ and 9.5%, 33.3% for Li_2MgH_4 respectively.

Owing to the superior efficiency and reliability, first-principles density functional theory (DFT) [14] has become a valuable tool in understanding properties of materials, predicting structures of unknown substances and interpreting experimental phenomena [15–17]. Especially, a variety of Li, Mg related hydrogen-storage materials have also been investigated based on it [18–21]. As to discover structures of novel materials, several first-principles computational methods have been employed. Database searching, simulated annealing, lattice cluster expansion are some commonly used ones [22]. Among these methods, the database mining approach is most widely used and believed sufficient to obtain accurate ground state energies reasonably. Recently, a series of theoretical predictions and studies of some alkali-containing ternary hydrides such as $ABeH_3$ [23], $AMgH_3$ [24], $ACaH_3$ [25] (A = Li, Na, K, Rb, and Cs) have been fulfilled by this method.

* Corresponding author. Tel.: +86 22 23506808; fax: +86 22 23506808.
E-mail address: chenabc@nankai.edu.cn (J. Chen).

0925-8388/$ – see front matter © 2011 Elsevier B.V. All rights reserved.
doi:10.1016/j.jallcom.2011.05.084

Researches of $LiMgH_3$ were once carried out based on the predicted pervoskite [26,27] and $LiTaO_3$-type [24] structures respectively. Since compounds such as Li_2BeH_4 [28] and K_2MgH_4 [29] have been discovered experimentally, we believe Li_2MgH_4 can also exist as an allotrope to $LiMgH_3$. In our work, we adapted the database mining approach not only to predict the structure of Li_2MgH_4 at the first time, but also to further test the controversial structure of $LiMgH_3$. Generally, Mg–Li alloy is believed to exist as an amorphous state. The phases of ordered magnesium–lithium alloys have been investigated via first-principles calculation lately [30]. We also extended our research to explore some other ordered Li–Mg–H phases derived from the ordered alloys. To thoroughly understand this Li–Mg–H ternary system, systematic analysis of the electronic and chemical bonding characters, as well as formation enthalpies based on the results of structural optimizations were then carried out.

2. Calculations

Our calculations are performed based on density functional theory (DFT) [14] as implemented in the Vienna *ab initio* simulation package (VASP) software [31] within a plane-wave basis set [32]. The interaction between ion and electron is described by the projector augmented wave method [33]. Perdew–Burke–Ernzerhof (PBE) projector-augmented wave pseudopotentials with semicore s and p states treated as valence were used [34]. The cutoff energy for plane waves in our calculations was 320 eV. Brillouin-zone integrations were performed on the 6*6*6 Monkhorst-Pack k-point mesh. To avoid the ambiguities regarding the free energy results, the same energy cutoff and a similar k-grid sampling for convergence were adopted.

During the structural optimizations, we deliberately break the symmetry of the input model down to triclinic *P1*. The ionic coordinates, size and shape of the unit cell were optimized simultaneously, and the relaxations were not stopped until the all the forces were less than 0.01 eV/Å.

The lattice vibrational calculations were carried out using the supercell method with finite displacements [35,36]. In this method, series of Hellmann–Feynman forces of a certain configuration with a single atom displaced from its equilibrium position are first calculated by VASP code. Calculations are performed in a relatively large supercell (in our work, the length of each edge is around 10 Å) with periodic boundary condition to avoid interactions between images of the displaced atom and guarantee the accuracy. The forces are collected to construct the force-constant matrices. The dynamical matrices are then solved to obtain phonon frequencies ω_i. Thus, the thermodynamic data of a specific substance, such as enthalpy and entropy, can be derived from the following formulae [20,37]:

$$H_{vib}(T) = \sum_i \frac{1}{2}\hbar\omega_i + \hbar\omega_i \left[\exp\left(\frac{\hbar\omega_i}{k_B T} - 1\right)\right]^{-1} \quad (1)$$

$$S_{vib}(T) = k_B \sum_i \frac{\hbar\omega_i / k_B T}{\exp(\hbar\omega_i / k_B T) - 1} - \ln\left[1 - \exp\left(-\frac{\hbar\omega_i}{k_B T}\right)\right] \quad (2)$$

3. Results and discussion

3.1. Structure optimization and analysis

The structure relaxation of Li_2MgH_4 has been performed based on 18 different potential structures with A_2BX_4 stoichiometric ratio. The proposed database is chosen following some principles. The searched structures are limited to chemically similar materials that have been reported by the Inorganic Crystal Structure Database (ICSD) [38]. Therefore, the possible elements A and B are confined to mono-valent and divalent metals from alkali, alkaline earth or transition metals separately, while X to hydrogen or halogen. In addition, some similar oxides are also included. The crystallographic structures inputted for calculations are namely (1) K_2MgH_4 (*I*4/*mmm*, tetragonal); (2) Rb_2MgH_4 (*Pnam*, orthogonal, also K_2ZnCl_4); (3) Na_2CuF_4 ($P2_1/c$, monoclinic); (4) Li_2MgCl_4 (*Fd*-3*m*, cubic, also Al_2MgO_4); (5) Rb_2CuCl_4 (*Cmca*, orthogonal, also La_2NiO_4); (6) Li_2MgBr_4 (*Cmmm*, orthogonal, also Li_2CoCl_4); (7) Na_2MgCl_4 (*Pbam*, orthogonal, also Na_2MnCl_4); (8) K_2BeF_4 ($Pna2_1$, orthogonal); (9) Li_2FeCl_4 (*Imma*, orthogonal); (10) Li_2CrCl_4 (*C*2/*m*, monoclinic); (11) K_2PtCl_4 (*P*4/*mmm*, tetragonal); (12) Li_2BeF_4 (*R*-3, trigonal); (13) Na_2PdCl_4 (*P*4/*ncc*, tetragonal); (14) K_2ZnBr_4 ($P2_1/m$, monoclinic); (15) β-Na_2SO_4 (*Fddd*, orthogonal); (16) K_2CoCl_4 ($P2_1/c$, monoclinic, also Na_2BeF_4); (17) Li_2ZnCl_4 (*Pnma*, orthogonal, also Cs_2MgCl_4); (18) Na_2BeF_4 ($Pn2_1a$, orthogonal, also Rb_2ZnCl_4). Though there are some structures belonging to the same space group, the differences of the number of atoms in the cell or the direction of crystalline axis lead them to divergent configurations and need to be considered separately. Among the crystal models imported for optimizations, the one with the lowest energy is Na_2MgCl_4-type, with *Pbam* space group and 28 atoms per unit cell. It can be regarded as the ground-state atomic arrangement of Li_2MgH_4 compound, the structure and parameter of which are shown in Fig. 1a and Table 1 respectively. The initial Na_2CuF_4 ($P2_1/C$) type candidate can also be relaxed to a similar structure as the Na_2MgCl_4 with only small variations in the positional parameters, which can be omitted. In addition, we got two competitive phases in energy with the ground state, *Imma* and *C*2/*m* respectively, the energies of which are within 10 kJ/mol per formula unit higher. The close energies of the above three bring on a big possibility of coexistence and conversion under some situations.

Following the searching principles stated above, we enumerate twelve possible structures for $LiMgH_3$, and those are (1) $KMgH_3$ (*Pm*3-*m*, cubic, also $LiBeH_3$); (2) $NaMgH_3$ (*Pnma*, orthogonal, also $KCaF_3$); (3) $LiTaO_3$ (*R*3*c*, trigonal); (4) $RbMgF_3$ (*P*63/*mmc*, hexagonal, also $CsMgCl_3$); (5) $KMgCl_3$ (*Pbnm*, orthogonal); (6) $FeTiO_3$ (*R*3-*m*, trigonal, also $NaMnCl_3$); (7) $NaMgF_3$ (*Cmcm*, orthogonal, also YBO_3); (8) $RbBeF_3$ ($P2_12_12_1$, orthogonal, also $KCuF_3$); (9) $RbCuF_3$ (*I*4/*mcm*, tetragonal); (10) $CsMgH_3$ (*R*3-*m*, trigonal, also $CsCoF_3$); (11) $KMnF_3$ (*P*4/*mbm*, tetragonal); (12) $RbCuCl_3$ (*Pbcn*, orthogonal). After relaxation, we get the same result as the one reported by Vajeeston that the lowest energy configuration for $LiMgH_3$ is $LiTaO_3$-type atomic arrangement [24]. Detailed structural information can be found in Fig. 1b and Table 1. However, it should be noted that the predicted structures for Li_2MgH_4 and $LiMgH_3$ is just for their ground state, the structural transformations along with pressure and temperature need to be further considered.

Based on the results of previous prediction, phonon vibration frequencies were then calculated, and no imaginary frequencies are observed, implying that both Na_2MgCl_4-type Li_2MgH_4 and $LiTaO_3$-type $LiMgH_3$ are dynamically stable. We then analyzed and discussed their structural features as follow. In the Li_2MgH_4, one Mg atom is surrounded by six H atoms. The Mg–H inter-atomic distances vary between 1.96 Å and 1.95 Å, and the H–Mg–H bond angles are very close to 90°. The two values above characterize that the MgH_6 arrangements in Li_2MgH_4 are regular octahedrons, different from the covalently BeH_4 or AlH_4 tetrahedrons in some Li–Be–H, Li–Al–H complex hydrides [23,39]. However, situations alter for Li–H coordination. There are also six H atoms around each Li, but the bond lengths are in a wide range from 1.90 Å to 2.14 Å and the H–Li–H bond angles from 78° to 116°. So the Li–H atomic arrangements can only be labeled as highly distorted octahedrons.

Similar analysis is done for the $LiMgH_3$ with *R*3*c* space group. The variation scopes for Mg–H and Li–H distances are from 1.91 Å to 2.00 Å and from 1.91 Å to 2.05 Å respectively. The H–Mg–H angles range between 80° and 101°, while H–Li–H angles between 77°

Table 1
Optimized equilibrium structural parameters for Li_2MgH_4 and $LiMgH_3$. The space group, number of formula units (Z), lattice and positional parameters are listed respectively.

Compound (space group)	Z	Lattice parameters (Å)	Positional parameters
Li_2MgH_4(*Pbam*)	2	a = 4.8968 b = 9.2532 c = 2.9185	Li(4*h*): 0.4821, 0.2096,0.5000 Mg(2*a*): 0.0000,0.0000,0.0000 H1(4*h*): 0.2078,0.9136,0.5000 H2(4*g*): 0.2183,0.1776,0.0000
$LiMgH_3$(*R*3*c*)	6	a = 4.9226 c = 13.2106	Li(6*a*): 0.0000,0.0000,0.2915 Mg(6*a*): 0.0000,0.0000,0.0013 H(18*b*): 0.0361,0.3641,0.0660

and 105°. In $LiMgH_3$, the MgH_6 and LiH_6 are both distorted octahedrons of similar shape. The bonding discrepancy of Li, Mg with H is smaller than that in Li_2MgH_4, due to the small proportion and less significant role of Li.

3.2. Chemical bonding

The prominent chemical bonding features can be identified by the calculated Electron Local Function (ELF) plots, as displayed in Fig. 2. The ELF values of the H sites are approximately equal to 1, while those of the Li, Mg sites are extreme low. The immense difference infers that few valence electrons are left to the metals during their interactions with H and the Li–Mg–H system mainly features an ionic property. However, the non-spherical contours of Mg, Li and H infer that covalent bond still exist in this system, especially between Mg and H. Bader charge analysis proves this judgment. The valence electrons of Li, Mg and H are 0.16, 0.42, and 1.82 respectively and the data are similar for both Li_2MgH_4 and $LiMgH_3$.

To understand the electronic properties of this system clearly, Li, Mg, H-partial and total density of states are calculated. It can be seen from Fig. 3 that both Li_2MgH_4 and $LiMgH_3$ are insulators with band gaps wider than 3.5 eV and behave similarly in chemical bonding. The valence band is primarily dominated by H s electrons and contributions from the other two are limited. It corresponds and confirms the ELF analysis above that the valence electrons have transferred from Li and Mg to H sites and thus, the bonds of Li–H and Mg–H possess predominantly ionic characters. Therefore, these ternary hydrides can also be conceived as insulating hydrogen crystals stabilized by metal atoms rather than as a mixed metal with H atoms [27].

In the valence bond region from −6 to −1 eV, Mg-s and Mg-p states are energetically separated and interact with H-s individually, while those of Li degenerate almost the whole scope. The details above indicate that the bonding features of Li and Mg with H are different, and some weak covalent bonds still exist between Mg and H. To some degree, the Mg–H interactions in these Li–Mg–H ternary complexes characterize a mixture of ionic and covalent components, just as the corresponding bonding natures in MgH_2 [40].

Nevertheless, another fact should not be neglected. There is no gap in the valence band region especially at −4 eV, reflecting that the Li–H and Mg–H interactions distribute broadly and continuously over the whole phase and this can be illustrated by the corner sharing connections of LiH_6 and MgH_6 octahedrons. Similar results also occur in some other simple hydrides, like the extended BeH_4 tetrahedrons in $LiBeH_3$ [23].

3.3. Thermodynamic properties and formation energies

The standard formation enthalpy at T = 0 K ($\Delta H^{T=0\,K}$), contains the electronic component (E_{el}) and ZPE (zero-point energy). Finite temperature contributions from lattice vibrations are further included. All the energies related to vibration are computed from the phonon density of states within the harmonic approximation [35]. The translational and rotational vibration modes are neglected for all solid reactants. The calculated zero point energy, enthalpies and entropies of substances involved in 300 K are listed in Table 2. As to Li, Mg, LiH and MgH_2, previous theoretical and experimental data are also shown. The differences of calculated vibrational enthalpies of 300 K and 0 K ($H_{vib}{}^{T=300\,K}$ − ZPE) correspond well with the values of $H^{T=300\,K} - H^{T=0\,K}$ in references. In addition, agreements

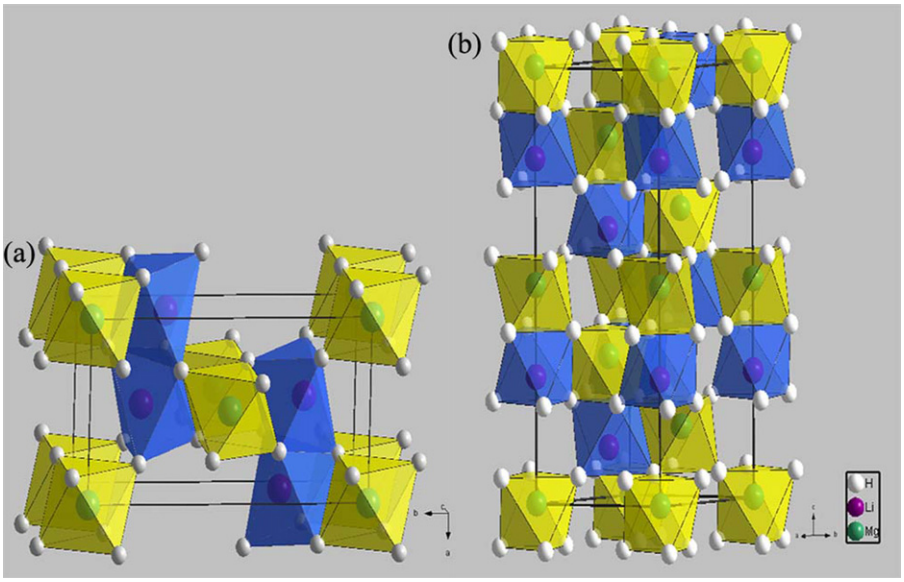

Fig. 1. The predicted crystal structures for Li_2MgH_4 (a) and $LiMgH_3$ (b).

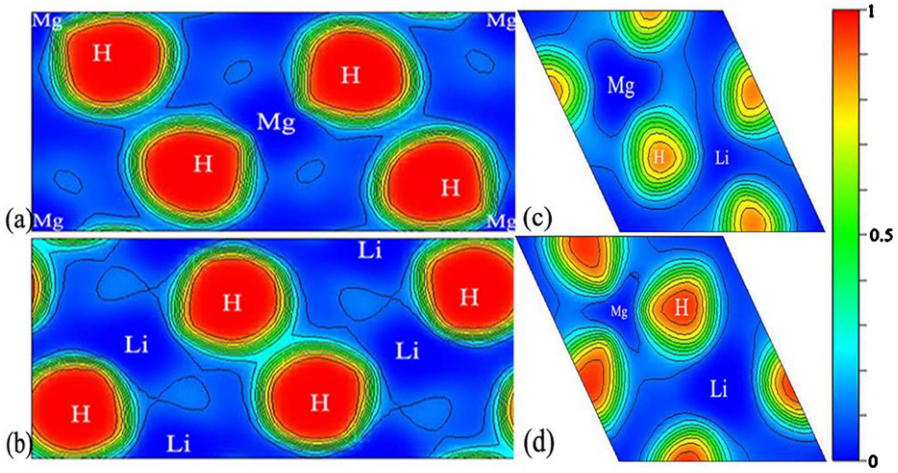

Fig. 2. ELF plots for different surfaces at [1 1 0] direction. (a) and (b) represent for surfaces of Li_2MgH_4 centered by Mg and Li atoms respectively, while (c) and (d) for those of $LiMgH_3$.

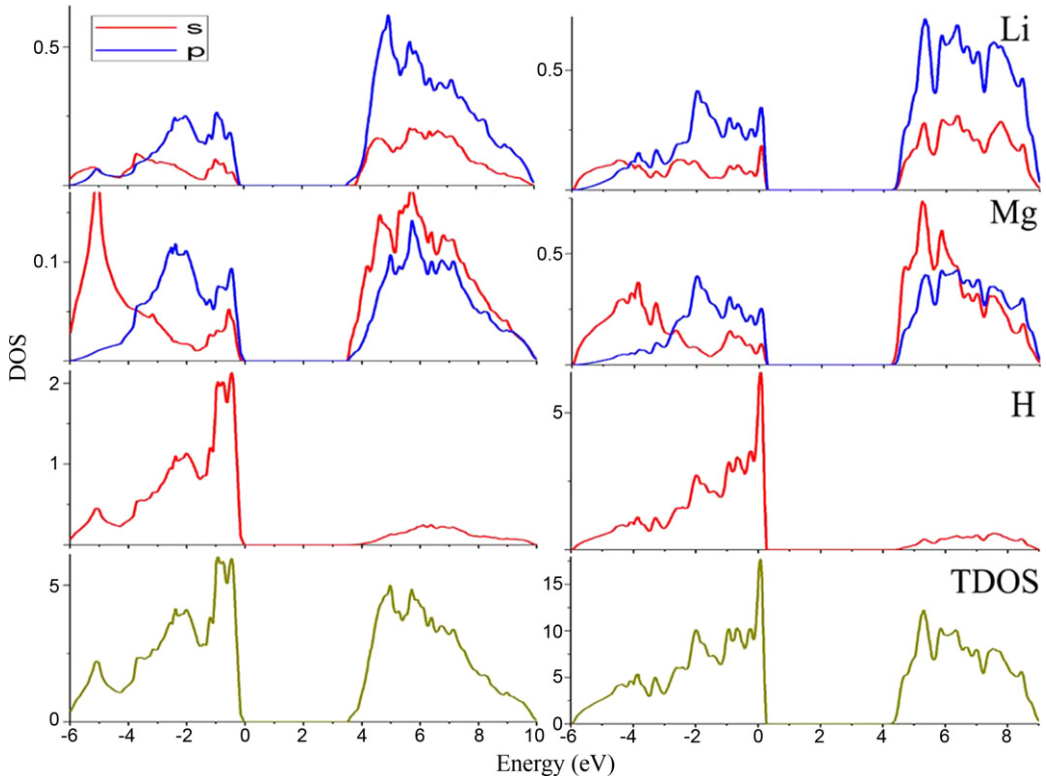

Fig. 3. Calculated partial (Li-s, Li-p, Mg-s, Mg-p, H-s) and total DOS for Li_2MgH_4 (left) and $LiMgH_3$ (right).

Table 2
Calculated thermodynamic data of substances related in this ternary system. Theoretical and experimental values of $H^{T=300\,K} - H^{T=0\,K}$ and $S^{T=300\,K}$ from references are respectively listed for comparison. ZPE refers to zero-point energy, also given by $H_{vib}{}^{T=0\,K}$. Units are kJ/mol f.u. for ZPE, $H_{vib}{}^{T=300\,K}$, $H^{T=300\,K} - H^{T=0\,K}$, and J/K/mol f.u. for $S_{vib}{}^{T=300\,K}$, $S^{T=300\,K}$.

System	Space group	ZPE($H_{vib}^{T=0\,K}$)	$H_{vib}^{T=300\,K}$	$H^{T=30\,K} - H^{T=0\,K}$ Ref. (theory/expt.[c])	$S_{vib}^{T=300\,K}$	$S^{T=300\,K}$ Ref. (theory/expt.[c])	Phonon supercell
Li	*Im*3-*m*	3.8	8.2	4.3[a]/4.7	28.0	27.7[b]/29.2	2*2*2
Mg	*P*63-*mmc*	2.9	7.9	5.0[a]/5.0	32.8	31.9[a]/32.8	3*3*2
LiH	*Fm*3-*m*	22.7	26.2	3.5[b]/3.8	17.7	17.7[b]/20.2	2*2*2
MgH_2	*P*42-*mnm*	39.9	45.4	5.4[a]/5.4	31.6	31.3[a]/31.9	3*3*4
Li_1Mg_1	*Pm*3-*m*	7.6	16.4		56.9		3*3*3
Li_1Mg_2	*Immm*	5.5	15.2		78.8		1*3*3
Li_2Mg_1	*Immm*	11.6	24.7		83.3		1*3*3
Li_2MgH_4	*Pbam*	80.6	94.5		78.8		2*1*3
$LiMgH_3$	*R*3*c*	61.4	70.6		52.0		1*2*1

[a] Calculated value from Ref. [16].
[b] Calculated value from Ref. [20].
[c] Experimental value from Ref. [41].

of the entropies are also reasonable. Treated as an ideal diatomic gas, the H_2 molecule is modeled by putting a H_2 dimer in a simple cubic supercell with a lattice constant 10 Å. Its internal energy is expressed as a sum of translational (3/2RT), rotational (RT) energies and the pV contribution to enthalpy is equal to RT. The zero-point energy used in our calculation is 25.7 kJ/mol [16]. The thread of our thermodynamic calculations is represented as follows and the data obtained are listed in Table 2.

$$\Delta E_{el} \xrightarrow{+\mathrm{ZPE}} \Delta H^{T=0\,\mathrm{K}} \xrightarrow[(\text{or molecular rotational+transitional+pV energy})]{+\text{finite temperature vibrational energy}} \Delta H^{T=300\,\mathrm{K}} \xrightarrow{-T\cdot\Delta S} \Delta G^{T=300\,\mathrm{K}}$$

As to the formation of the Li–Mg–H ternary hydrides, five possible pathways are considered in this study. Besides the LiH, MgH_2, Li, Mg, we also include the ordered Li–Mg alloy phase [30] as a potential reactant. Combining the electronic and vibrational energies calculated above, ambient temperature formation Gibbs free energy ($\Delta G^{T=300\,\mathrm{K}}$) of Li_2MgH_4 (*Pbam*) and $LiMgH_3$ (*R*3*c*) for different reaction equations are derived and summarized in Table 3.

The data in Table 3 reveal that all the reaction pathways are exothermic. The reaction starting from elementary substances, as well as the predicted ordered alloy phases, seems to be a large energy liberation process and can be taken as a guide for preparation of these ternary hydrides. From the point of view of energy, there is a big possibility for the predicted $LiMgH_3$ and Li_2MgH_4 to form in equilibrium conditions. However, the high energetic barriers for cation diffusion within the solid phases forbid the combination and separation of phases kinetically at ambient conditions [18]. Thus, the pure phase is not easy to get by a straightforward combination of Li, Mg and H_2. Separations of the ordered hydride from amorphous solid solution may require extra experimental conditions such as an extreme temperature and pressure or a relatively long operating time. The specific kinetic limitation needs to be investigated thoroughly. Nevertheless, a series of $MMgH_3$ or M_2MgH_4 (M = Na [42], Rb [43], Cs [44]) compounds have been prepared by corresponding binary hydrides experimentally. Considering the formation Gibbs free energy of pathway (3) close to 0 kJ/mol, reversible decompositions of $LiMgH_3$ or Li_2MgH_4 to LiH and MgH_2 seem to be favorable thermodynamically. It may explain why the Li–Mg–H ternary hydride with pure and single phase has not yet been founded this way experimentally. In reality, the formation processes of these ternary hydrides may include some other compounds as intermediates and be multiple-step reactions. It can be concluded that the regular Li–Mg–H ternary compounds cannot be synthesized easily. Though pathways of (1) and (3) can be taken as potential preparation pathways, actual limitations from kinetics and thermodynamics have to be overcome respectively. Moreover, in practice, the energy reduction contributed by defects and mixing entropy will further prevent the pure ordered compounds to be stabilized.

3.4. Inserting H atoms into the predicted ordered Li–Mg alloy

The potential ordered Li–Mg alloy phases have recently been reported by Taylor et al. using cluster expansion method [30]. They are Li_1Mg_1, Li_1Mg_2 and Li_2Mg_1, with space groups *Pm*-3*m*, *Immm*, and *Immm* respectively. We further do an electronic analysis of these structures. The structures and corresponding ELF plots of these three are shown in Fig. 4a, c, and f.

As the ELF pictures display, all of these Li–Mg alloys have regions of high ELF values approximate to 1, indicating that electrons are excluded by metals and highly located in these areas. Generally, H prefers to stay at the interstitial sites where electrons have relatively more non-bonding localized nature than other possible sites in metal matrices [45]. The spaces with high electron density thus tend to be occupied by H atoms to form other ordered Li–Mg–H ternary hydrides.

We studied the H uptake behavior of the ordered Li–Mg alloy through sequential insertion of H atoms. The sites with ELF values higher than 0.8 are first taken into consideration as promising host for H atoms. Three H atoms are located at the face center of Li_1Mg_1 to obtain a perovskite structure, which was once considered as an ideal arrangement for $LiMgH_3$ [26,27]. No extra free electron distributions are identified by the ELF plots after the H insertion. However, it should be noted that though this *Pm*3-*m* type $LiMgH_3$ appears to be rational in terms of spatial and electronic distribution, its energy is much higher than the previously predicted $LiTaO_3$ (*R*3*c*) type and has imaginary frequencies with a dynamically instability. This structure may exist as an ordered phase at some certain external condition and further confirmation needs to be taken experimentally and theoretically.

Two H atoms are put into the Li_1Mg_2 and formed $Li_2Mg_4H_2$ (*Imm*2), as seen in Fig. 4c. Li_2Mg_1 gets four H atoms and the resulted $Li_4Mg_2H_4$ is also *Imm*2, as seen in Fig. 4f. Density of state (DOS) of the $Li_2Mg_4H_2$ and $Li_4Mg_2H_4$ have been calculated, and both have Fermi-levels around 3.5 eV and no band gaps, thus they should be classified as conductors unlike the $LiMgH_3$ and Li_2MgH_4 analyzed above. This feature is also observed by their ELF plots and can be ascribed to the large amount of vacancies and electrons still left unoccupied. Thus, the systems have properties much like the binary alloys they derived from and could accommodate some more H atoms. As a result, H atoms are continued to put into other sites of the $Li_2Mg_4H_2$ and $Li_4Mg_2H_4$ with relatively high ELF values to reach the saturated stoichiometric ratio. Thus, we get the $Li_2Mg_4H_{10}$ and $Li_4Mg_2H_8$ with configurations and charge distributions (Fig. 4e and h). The system ultimately reaches its insulating state after H loading stepwise. Their electronic properties are just like the ground state structures analyzed above. However, from the Phonon DOS calculations, imaginary frequencies are both observed, implying that these predicted structures are dynamically unstable, unlike the others illustrated before. It can be inferred that both structures are metastable and once after formation may convert to some other Li–Mg–H ternary phases or, with much bigger possibility, break down to MgH_2 and LiH, since the Gibbs free energy of this route is close to zero even for the predicted ground state ternary hydrides.

Table 3
Formation enthalpies of Li_2MgH_4 (*Pbam*) and $LiMgH_3$ (*R*3*c*) at *T* = 300 K with respect to different reaction pathways.

Formation equation	$\Delta G^{T=300\,\mathrm{K}}$ (kJ/mol)	Formation equation	$\Delta G^{T=300\,\mathrm{K}}$ (kJ/mol)
(1) $2Li + Mg + 2H_2 \rightarrow Li_2MgH_4$	−215.6	$Li + Mg + (3/2)H_2 \rightarrow LiMgH_3$	−129.7
(2) $Li_2Mg_1 + 2H_2 \rightarrow Li_2MgH_4$	−203.7	$LiMg + (3/2)H_2 \rightarrow LiMgH_3$	−126.0
(3) $2LiH + MgH_2 \rightarrow Li_2MgH_4$	−28.3	$LiH + MgH_2 \rightarrow LiMgH_3$	−10.5
(4) $2Li + MgH_2 + H_2 \rightarrow Li_2MgH_4$	−163.6	$Li + MgH_2 + (1/2)H_2 \rightarrow LiMgH_3$	−78.1
(5) $2LiH + Mg + H_2 \rightarrow Li_2MgH_4$	−80.0	$LiH + Mg + H_2 \rightarrow LiMgH_3$	−62.1

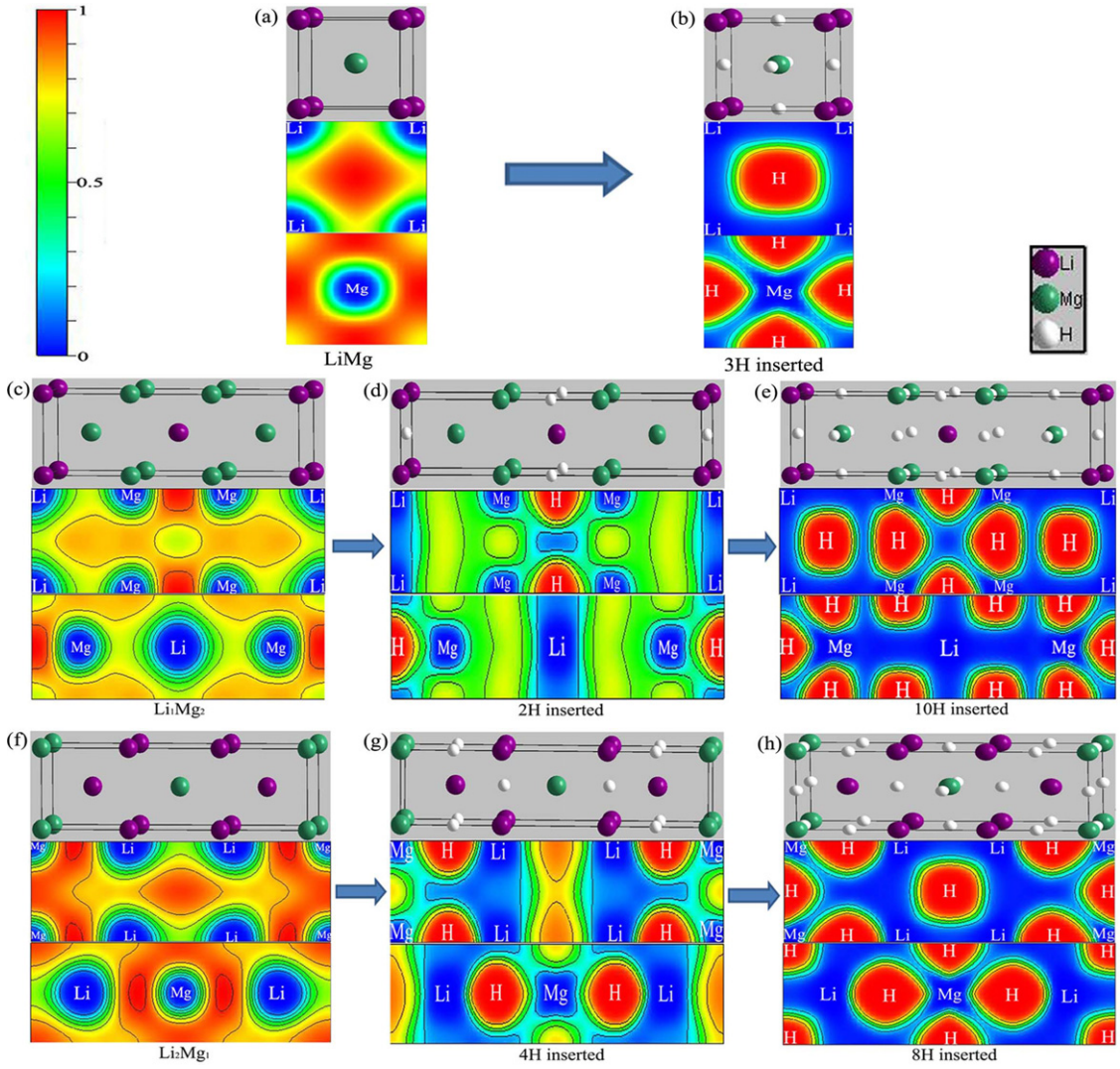

Fig. 4. Structures and corresponding (0 0 1) and (0 0 2) surface ELF plots of the ordered Li–Mg alloys and substances resulted by proper H insertion.

4. Conclusions

A structural, electronic, and thermodynamic study of the ordered Li–Mg–H system has been performed in detail based on DFT. Closely related structures of different space groups have been imposed as the database for searching the ground state structures of Li_2MgH_4 and $LiMgH_3$. The resulted structures after relaxations are *Pbam* (Na_2MgCl_4 type) and *R*3*c* ($LiTaO_3$ type) respectively, composed of LiH_6 and MgH_6 octahedrons connecting each other by corner sharing. According to electronic and chemical bonding analysis, the Li–Mg–H compounds are insulators and dominated by ionic bonds in addition to some covalent component between Mg and H. Finite temperature thermodynamic data corresponding to different formation routes are compared. Preparations through Li, Mg and H_2 are energetically favorable, but may be inhabited kinetically by pure phase separation. The actual formation process for the pure, ordered phase should be exploited under some special experimental conditions. The decomposition to LiH and MgH_2 not only limits the thermodynamic feasibility of synthesis by combining these binary hydrides but can also explain the difficulty to discover these order ternary phases. Inserting H atoms into the sites of ordered Li–Mg alloy phases with high electronic density has been taken as another way to discover proper Li–Mg–H phase. The H-uptaken derivations appear to be rational with respect to spatial and electronic distributions. Systems derived from Li_1Mg_2 and Li_2Mg_1 display a conversion from conductors to insulators as H uptakes consequently. However, when saturated by H to the stoichiometric ratio, imaginary frequencies are observed in these substances, indicating the dynamically instability.

Acknowledgements

This work was supported by the Research Programs of National NSFC (20873071), MOST (2009AA03Z224 and 2010CB631301), MOE Innovation Team (IRT0927), and Tianjin High-Tech (10ZCGHHZ01200).

References

[1] P. Chen, M. Zhu, Mater. Today 11 (2008) 36.
[2] B. Peng, J. Chen, Coord. Chem. Rev. 253 (2009) 2805.
[3] I.P. Jain, P. Jain, A. Jain, J. Alloys Compd. 503 (2010) 303.
[4] Y. Wang, S. Liu, L. Rong, Y. Wang, J. Phys.: Condens. Matter 22 (2010) 175502.
[5] T. Noritake, M. Aoki, M. Matsumoto, K. Miwa, S. Towata, H. Li, S. Orimo, J. Alloys Compd. (2011), doi:10.1016/j.jallcom.2011.04.079.
[6] Y. Liu, C. Liang, Z. Wei, Y. Jiang, M. Gao, H. Pan, Q. Wang, Phys. Chem. Chem. Phys. 12 (2010) 3108.
[7] L. Li, B. Peng, Z. Tao, F. Cheng, J. Chen, Adv. Funct. Mater. 20 (2010) 1894.
[8] J. Mao, Z. Guo, X. Yu, H. Liu, J. Alloys Compd. 509 (2011) 5012.
[9] Z. Fang, X. Kang, P. Wang, H. Li, S. Orimo, J. Alloys Compd. 491 (2010) L1.

[10] J. Chen, F. Cheng, Acc. Chem. Res. 42 (2009) 713.
[11] M.R. Palacin, Chem. Soc. Rev. 38 (2009) 2565.
[12] Y. Oumellal, A. Rougier, G.A. Nazri, J.M. Tarascon, L. Aymard, Nat. Mater. 7 (2008) 916.
[13] Y. Oumellal, A. Rougier, J.M. Tarascon, L. Aymard, J. Power Sources 192 (2009) 698.
[14] W. Kohn, L.J. Sham, Phys. Rev. 140 (1965) A1133.
[15] F. Cheng, J. Shen, B. Peng, Y. Pan, Z. Tao, J. Chen, Nat. Chem. 3 (2011) 79.
[16] A.R. Akbarzadeh, V. Ozoliņš, C. Wolverton, Adv. Mater. 19 (2007) 3233.
[17] B. Peng, F. Cheng, Z. Tao, J. Chen, J. Chem. Phys. 133 (2010) 034701.
[18] K.C. Smith, T.S. Fisher, U.V. Waghmare, R. Grau-Crespo, Phys. Rev. B 82 (2010) 134109.
[19] B. Peng, L. Li, W. Ji, F. Cheng, J. Chen, J. Alloys Compd. 484 (2009) 308.
[20] D.J. Siegel, C. Wolverton, V. Ozoliņš, Phys. Rev. B 75 (2007) 014101.
[21] L. Li, B. Peng, W. Ji, J. Chen, J. Phys. Chem. C 113 (2009) 3007.
[22] C. Wolverton, D.J. Siegel, A.R. Akbarzadeh, V. Ozoliņš, J. Phys.: Condens. Matter 20 (2008) 064228.
[23] P. Vajeeston, P. Ravindran, H. Fjellvåg, Inorg. Chem. 47 (2007) 508.
[24] P. Vajeeston, P. Ravindran, A. Kjekshus, H. Fjellvåg, J. Alloys Compd. 450 (2008) 327.
[25] P. Vajeeston, P. Ravindran, H. Fjellvåg, J. Chem. Phys. 132 (2010) 114504.
[26] Y. Li, B. Rao, T. McMullen, P. Jena, P.K. Khowash, Phys. Rev. B 44 (1991) 6030.
[27] B. Pfrommer, C. Elsässer, M. Fähnle, Phys. Rev. B 50 (1994) 5089.
[28] A. Zaluska, L. Zaluski, J.O. Ström-Olsen, J. Alloys Compd. 307 (2000) 157.
[29] B. Bertheville, T. Herrmannsdörfer, K. Yvon, J. Alloys Compd. 325 (2001) L13.
[30] R.H. Taylor, S. Curtarolo, G.L.W. Hart, Phys. Rev. B 81 (2010) 024112.
[31] G. Kresse, J. Hafner, Phys. Rev. B 47 (1993) 558.
[32] G. Kresse, J. Furthmüller, Comput. Mater. Sci. 6 (1996) 15.
[33] P.E. Blöchl, Phys. Rev. B 50 (1994) 17953.
[34] G. Kresse, D. Joubert, Phys. Rev. B 59 (1999) 1758.
[35] A. Togo, F. Oba, I. Tanaka, Phys. Rev. B 78 (2008) 134106.
[36] G.J. Ackland, J. Phys.: Condens. Matter 14 (2002) 2975.
[37] D.C. Wallace, Thermodynamics of Crystals, John Wiley & Sons, New York, 1972.
[38] Inorganic Crystal Structure Database, Gmelin Institut, Germany, 2006.
[39] O.M. Løvvik, S.M. Opalka, H.W. Brinks, B.C. Hauback, Phys. Rev. B 69 (2004) 134117.
[40] T. Noritake, M. Aoki, S. Towata, Y. Seno, Y. Hirose, E. Nishibori, M. Takata, M. Sakata, Appl. Phys. Lett. 81 (2002) 2008.
[41] M.W. Chase Jr., NIST-JANAF Thermochemical Tables, 4th ed., American Chemical Society, Washington, DC, 1998.
[42] E. Rönnebro, D. Noréus, K. Kadir, A. Reiser, B. Bogdanovic, J. Alloys Compd. 299 (2000) 101.
[43] F. Gingl, T. Vogt, E. Akiba, K. Yvon, J. Alloys Compd. 282 (1999) 125.
[44] B. Bertheville, P. Fischer, K. Yvon, J. Alloys Compd. 330–332 (2002) 152.
[45] P. Vajeeston, P. Ravindran, R. Vidya, A. Kjekshus, H. Fjellvåg, Europhys. Lett. 72 (2005) 569.